RSC Advances

PAPER

View Article Online
View Journal | View Issue

Cite this: *RSC Adv.*, 2017, **7**, 21592

Bicyclic ammonium ionic liquids as dense hypergolic fuels†

Yutao Yuan,[ab] Yanqiang Zhang,*[a] Long Liu,[a] Nianming Jiao,[ab] Kun Dong[a] and Suojiang Zhang*[a]

It is critical for hypergolic fuels to be dense so as to enhance the performance of propellants and improve the loading of rockets. Considering that dense elements and bicyclic rings contribute to high density, two series of ionic liquids were prepared with 1-aza-bicyclo[2.2.2]octane-/1,4-diazabicyclo[2.2.2]octane-based cations and the dicyanamide anion. Their key properties were measured or calculated as decomposition temperature (208–322 °C), density (1.06–1.31 g cm^{-3}), specific impulse (260.5 to 266.2 s) and ignition delay time (14–1053 ms). Compared with 1-aza-bicyclo[2.2.2]octane-based ionic liquids, the corresponding 1,4-diazabicyclo[2.2.2]octane-based ionic liquids exhibit a lower decomposition temperature, higher density and bigger specific impulse. As expected, 1-methyl-1-azonia-bicyclo[2.2.2]octane and 1-(prop-2-ynyl)-4-aza-1-azonia-bicyclo[2.2.2]octane dicyanamide possess higher densities (1.20 and 1.19 g cm^{-3}) than the corresponding pyrrolidinium and imidazolium-based isomers (1.05 and 1.07 g cm^{-3}), besides hypergolicity with white fuming nitric acid.

Received 15th March 2017
Accepted 9th April 2017

DOI: 10.1039/c7ra03090h

rsc.li/rsc-advances

Introduction

Hypergolic bipropellants are mainly composed of an energetic fuel and a strong oxidizer.[1] The fuel–oxidizer combinations can simplify engine design and guarantee thousands of ignitions so as to be highly reliable for space crafts during their long lifetime. As to the fuels, hydrazine derivatives with high specific impulse, short ignition delay time and super thrust control, have been widely applied in rockets.[2] Although having high performance, hydrazine derivatives are becoming less and less favorable as propellant fuels because of their high volatility and carcinogenicity.[3–5] With the enhancement of environmental awareness, it has been an urgent task to develop green alternatives of hydrazine derivatives. Fortunately, energetic ionic liquids (ILs) possess corresponding advantages such as negligible vapor pressure, low toxicity and high thermal/chemical stability, and have potential as candidates of green propellant fuels.

In 2008, the Air Force Research Laboratory reported a series of dicyanamide-based ILs, which first demonstrated that ILs could be spontaneously ignited with white fuming nitric acid (WFNA) and N_2O_4.[6,7] Since then, hypergolic ILs have gained increasing attention, and become a scientific frontier of propellants.[8,9] Considering that the anions could play a key role in ignitions, a lot of hypergolic ILs with different anions have been prepared, such as $N(CN)_2^-$,[8] BH_4^-,[10] BH_3CN^-,[11] $BH_2(CN)_2^-$,[12–14] *etc.* Most of these studies are focused on shortening the ignition delay times (t_{id}) of ILs.[15–18] However, as hypergolic propellant fuels, it is critical for them to be dense, which not only increases specific impulse (I_{sp}) values, but also improves efficient fuel loading in rockets. With common cations (imidazolium, pyrrolidinium, pyridinium), densities of BH-based ILs (including BH_4^-, BH_3CN^- and $BH_2(CN)_2^-$) are all lower than 1.03 g cm^{-3},[10–14] and densities NCN-based ILs ($N(CN)_2^-$) are not more than 1.165 g cm^{-3}.[19] Up to now, how to boost the densities of hypergolic ILs is relatively neglected.

In this work, we designed the molecular structures of dense hypergolic ILs following the two basic rules. One is to add the heavy elements to IL molecules. Compared with B atom (diameter, 0.88 Å; relative mass, 10.81; electronegativity, 2.04), N atom is smaller (diameter, 0.74 Å), heavier (relative mass, 14.01) and stronger (electronegativity, 3.04). Thus, the N-based anion ($N(CN)_2^-$) was selected rather than B-based anions (BH_4^-, BH_3CN^-, $BH_2(CN)_2^-$) in targeted ILs. The other is to form polycyclic rings in IL molecules. The tension of polycyclic rings can shorten the bond lengths so as to make the targeted molecules denser. Based on the above two ideas, we synthesized 1-aza-bicyclo[2.2.2]octane-based (ABCO) and 1,4-diazabicyclo[2.2.2]octane-based (DABCO) ILs. The structures of ILs were confirmed by NMR, IR spectroscopies, and electrospray ionization mass spectrometry (ESI-MS). The properties of ILs were fully discussed also. Indeed, these ILs exhibit higher densities

[a]*Division of Ionic Liquids and Green Engineering, Institute of Process Engineering, Chinese Academy of Sciences, Beijing 100190, China. E-mail: yqzhang@ipe.ac.cn; sjzhang@ipe.ac.cn; Fax: +86-10-82544875*

[b]*School of Chemistry and Chemical Engineering, University of Chinese Academy of Sciences, Beijing 100049, China*

† Electronic supplementary information (ESI) available. CCDC 1509452. For ESI and crystallographic data in CIF or other electronic format see DOI: 10.1039/c7ra03090h

than the corresponding pyrrolidinium-/imidazolium-based ILs, besides hypergolicity with WFNA.

Experimental

Caution

Although none of the compounds described herein has exploded or detonated in the course of this research, these materials should be handled with extreme care by using the best safety practices.

General methods

All of the analytical reagents were purchased from commercial sources and were used as received. ^{1}H and ^{13}C NMR spectra were recorded using a Bruker AVANCE III 600 MHz nuclear magnetic resonance spectrometer operating at 600 or 151 MHz, respectively. All NMR spectra were used [D_6]DMSO as solvent. Chemical shifts are reported relative to Me_4Si. The melting and decomposition points were recorded using a Mettler-Toledo DSC1 differential scanning calorimeter (DSC) at a scan rate of 10 °C min^{-1} in closed aluminum containers. Infrared spectra were obtained by using KBr pellets with a Thermo Nicolet 380 infrared spectroscopy. Density and viscosity of the hypergolic ILs were measured at 25 °C by using a DMA 5000-AMVn Anton Paar viscometer. High resolution mass spectra of ILs were recorded on a Bruker QTOF mass spectrometer.

Preparation of precursors 1–8

The precursors of **1–4** were synthesized and purified according to literature procedures.[20] The precursors **5–8** were synthesized based on other published routes.[21–24]

General procedure for preparation of 9–16

Precursors **1–8** (20.0 mmol) was dissolved in CH_3OH (25 mL), and a suspension of $AgN(CN)_2$ (22.0 mmol) in CH_3OH (25 mL) was added. After stirring at room temperature for 4 h, the insoluble silver halide was removed by filtration. The filtrate was concentrated using a rotary evaporator, and then dried under vacuum to yield crude product. The crude product was dissolved in CH_2Cl_2 (20 mL) with stirring for 1 h. After stored at room temperature for another 3 h, the resulting solution was filtered again. The filtrate was evaporated to remove CH_2Cl_2 by using a rotary evaporator, and dried under vacuum at 70 °C to obtain final product.

1-Methyl-1-azonia-bicyclo[2.2.2]octane dicyanamide (9a). Yield, 97.3%; white solid; ^{1}H NMR (600 MHz, [D_6]DMSO): δ = 1.85 (m, 6H; CH_2), 2.06 (m, H; CH), 2.88 (s, 3H; CH_3), 3.38 ppm (t, 6H; CH_2); ^{13}C NMR (151 MHz, [D_6]DMSO): δ = 18.74, 23.50, 51.37, 55.92, 119.15 ppm; IR (KBr): $\tilde{\nu}$ = 3449, 2961, 2886, 2238, 2209, 2135, 1648, 1492, 1469, 1383, 1339, 1122, 952, 832, 523 cm^{-1}; HRMS (ESI): *m*/*z* calcd for cation $C_8H_{16}N^+$: 126.1277 $[M]^+$, found: 126.1243; *m*/*z* calcd for $C_2N_3^-$: 66.0098 $[M]^-$, found: 66.0094.

1-Ethyl-1-azonia-bicyclo[2.2.2]octane dicyanamide (10a). Yield, 96.6%; colorless liquid; ^{1}H NMR (600 MHz, [D_6]DMSO): δ = 1.19 (t, 3H; CH_3), 1.85 (s, 6H; CH_2), 2.06 (m, H; CH), 3.15 (m, 2H; CH_2), 3.33 ppm (t, 6H; CH_2); ^{13}C NMR (151 MHz, [D_6]DMSO): δ = 7.43, 19.13, 23.35, 53.23, 58.63, 119.18 ppm; IR (KBr): $\tilde{\nu}$ = 3442, 2958, 2886, 2235, 2196, 2136, 1464, 1313, 1106, 1094, 961, 523 cm^{-1}; HRMS (ESI): *m*/*z* calcd for cation $C_9H_{18}N^+$: 140.1434 $[M]^+$, found: 140.1400; *m*/*z* calcd for $C_2N_3^-$: 66.0098 $[M]^-$, found: 66.0096.

1-Propyl-1-azonia-bicyclo[2.2.2]octane dicyanamide (11a). Yield, 93.5%; white solid; ^{1}H NMR (600 MHz, [D_6]DMSO): δ = 0.88 (t, 3H; CH_3), 1.65 (m, 2H; CH_2), 1.85 (s, 6H; CH_2), 2.06 (t, H; CH), 3.04 (m, 2H; CH_2), 3.35 ppm (t, 6H; CH_2); ^{13}C NMR (151 MHz, [D_6]DMSO): δ = 10.77, 15.01, 19.05, 23.40, 53.77, 64.71, 119.17 ppm; IR (KBr): $\tilde{\nu}$ = 3496, 2956, 2879, 2234, 2192, 2135, 1494, 1461, 1346, 1313, 1099, 974, 923, 835, 753, 517 cm^{-1}; HRMS (ESI): *m*/*z* calcd for cation $C_{10}H_{20}N^+$: 154.1590 $[M]^+$, found: 154.1601; *m*/*z* calcd for $C_2N_3^-$: 66.0098 $[M]^-$, found: 66.0094.

1-Butyl-1-azonia-bicyclo[2.2.2]octane dicyanamide (12a). Yield, 98.6%; colorless liquid; ^{1}H NMR (600 MHz, [D_6]DMSO): δ = 0.92 (t, 3H; CH_3), 1.27 (m, 2H; CH_2), 1.61 (m, 2H; CH_2), 1.85 (s, 6H; CH_2), 2.05 (t, H; CH), 3.08 (t, 2H; CH_2), 3.35 ppm (t, 6H; CH_2); ^{13}C NMR (151 MHz, [D_6]DMSO): δ = 13.52, 19.08, 19.42, 23.40, 53.74, 63.09, 119.16 ppm; IR (KBr): $\tilde{\nu}$ = 2961, 2882, 2233, 2194, 2133, 1647, 1493, 1465, 1386, 1311, 1212, 1095, 971, 937, 835, 523 cm^{-1}; HRMS (ESI): *m*/*z* calcd for cation $C_{11}H_{22}N^+$: 168.1747 $[M]^+$, found: 168.1762; *m*/*z* calcd for $C_2N_3^-$: 66.0098 $[M]^-$, found: 66.0100.

1-Allyl-1-azonia-bicyclo[2.2.2]octane dicyanamide (13a). Yield, 96.0%; brown liquid; ^{1}H NMR (600 MHz, [D_6]DMSO): δ = 1.86 (s, 6H; CH_2), 2.07 (t, H; CH), 3.35 (t, 6H; CH_2), 3.78 (d, 2H; CH_2), 5.58 (m, 2H; CH_2), 5.98 ppm (m, H; CH); ^{13}C NMR (151 MHz, [D_6]DMSO): δ = 19.39, 23.37, 53.85, 65.32, 119.18, 125.61, 127.14 ppm; IR (KBr): $\tilde{\nu}$ = 3446, 3016, 2959, 2858, 2235, 2195, 2135, 1466, 1429, 1308, 1312, 1084, 1015, 956, 892, 835, 649, 523 cm^{-1}; HRMS (ESI): *m*/*z* calcd for cation $C_{10}H_{18}N^+$: 152.1434 $[M]^+$, found: 152.1454; *m*/*z* calcd for $C_2N_3^-$: 66.0098 $[M]^-$, found: 66.0084.

1-(Prop-2-ynyl)-1-azonia-bicyclo[2.2.2]octane dicyanamide (14a). Yield, 94.3%; brown solid; ^{1}H NMR (600 MHz, [D_6]DMSO): δ = 1.90 (s, 6H; CH_2), 2.08 (t, H; CH), 3.44 (t, 6H; CH_2), 4.05 (s, H; CH), 4.20 ppm (d, 2H; CH_2); ^{13}C NMR (151 MHz, [D_6]DMSO): δ = 19.02, 23.34, 52.83, 54.12, 72.20, 83.40, 119.16 ppm; IR (KBr): $\tilde{\nu}$ = 3504, 3233, 3151, 3019, 3002, 2960, 2886, 2240, 2194, 2134, 1496, 1464, 1318, 1204, 1121, 923, 892, 833, 714, 663, 521 cm^{-1}; HRMS (ESI): *m*/*z* calcd for cation $C_{10}H_{16}N^+$: 150.1277 $[M]^+$; found: 150.1293 *m*/*z* calcd for $C_2N_3^-$: 66.0098 $[M]^-$; found: 66.0093.

1-(Cyanomethyl)-1-azonia-bicyclo[2.2.2]octane dicyanamide (15a). Yield, 97.1%; white solid; ^{1}H NMR (600 MHz, [D_6]DMSO): δ = 1.92 (d, 6H; CH_2), 2.10 (t, H; CH), 3.54 (t, 6H; CH_2), 4.71 ppm (s, 2H; CH_2); ^{13}C NMR (151 MHz, [D_6]DMSO): δ = 18.54, 23.25, 50.60, 55.54, 111.92, 119.16 ppm; IR (KBr): $\tilde{\nu}$ = 3355, 2957, 2885, 2287, 2242, 2199, 2141, 1647, 1492, 1465, 1384, 1322, 1211, 1104, 1086, 1045, 960, 833, 667, 525 cm^{-1}; HRMS (ESI): *m*/*z* calcd for cation $C_9H_{15}N_2^+$: 151.1230 $[M]^+$, found: 151.1253 *m*/*z* calcd for $C_2N_3^-$: 66.0098 $[M]^-$, found: 66.0091.

1-(2-Hydroxyethyl)-1-azonia-bicyclo[2.2.2]octane dicyanamide (16a). Yield, 95.2%; white solid; ^{1}H NMR (600 MHz, [D_6]DMSO):

δ = 1.85 (s, 6H; CH_2), 2.05 (t, H; CH), 3.21 (t, 2H; CH_2), 3.45 (t, 6H; CH_2), 3.80 (d, 2H; CH_2), 5.23 ppm (t, H; CH); ^{13}C NMR (151 MHz, [D_6]DMSO): δ = 19.12, 23.45, 54.49, 54.62, 65.23, 119.16 ppm; IR (KBr): $\tilde{\nu}$ = 3491, 3014, 2978, 2934, 2888, 2234, 2195, 2131, 1409, 1466, 1425, 1384, 1308, 1254, 1112, 994, 925, 833, 517 cm^{-1}; HRMS (ESI): *m*/*z* calcd for cation $C_9H_{18}NO^+$: 156.1383 $[M]^+$, found: 156.1412 *m*/*z* calcd for $C_2N_3^-$: 66.0098 $[M]^-$, found: 66.0085.

1-Methyl-4-aza-1-azonia-bicyclo[2.2.2]octane dicyanamide (9b). Yield, 88.5%; white solid; ^{1}H NMR (600 MHz, [D_6]DMSO): δ = 2.95 (s, 3H; CH_3), 3.02 (t, 6H; CH_2), 3.25 ppm (t, 6H; CH_2); ^{13}C NMR (600 MHz, [D_6]DMSO): δ = 44.61, 50.73, 53.22, 118.99 ppm; IR (KBr): $\tilde{\nu}$ = 2249, 2204, 2145, 1470, 1384, 1324, 1055, 840, 794, 692, 521 cm^{-1}; HRMS (ESI): *m*/*z* calcd for cation $C_7H_{15}N_2^+$: 127.1230 $[M]^+$, found: 127.1245; *m*/*z* calcd for $C_2N_3^-$: 66.0098 $[M]^-$, found: 66.0063.

1-Ethyl-4-aza-1-azonia-bicyclo[2.2.2]octane dicyanamide (10b). Yield, 94.1%; colorless liquid; ^{1}H NMR (600 MHz, [D_6]DMSO): δ = 1.22 (t, 3H; CH_3), 3.02 (t, 6H; CH_2), 3.24 ppm (m, 8H; CH_2); ^{13}C NMR (600 MHz, [D_6]DMSO): δ = 7.07, 44.64, 51.02, 58.67, 119.08 ppm; IR (KBr): $\tilde{\nu}$ = 2960, 2231, 2193, 2133, 1462, 1377, 1309, 1056, 994, 884, 843, 795, 673, 525 cm^{-1}; HRMS (ESI): *m*/*z* calcd for cation $C_8H_{17}N_2^+$: 141.1386 $[M]^+$, found: 141.1374; *m*/*z* calcd for $C_2N_3^-$: 66.0098 $[M]^-$, found: 66.0062.

1-Propyl-4-aza-1-azonia-bicyclo[2.2.2]octane dicyanamide (11b). Yield, 94.4%; white solid; ^{1}H NMR (600 MHz, [D_6]DMSO): δ = 0.91 (t, 3H; CH_3), 1.67 (m, 2H; CH_2), 3.02 (t, 6H; CH_2), 3.12 (m, 2H; CH_2), 3.25 ppm (t, 6H; CH_2); ^{13}C NMR (600 MHz, [D_6] DMSO): δ = 10.62, 14.63, 44.66, 51.56, 64.66, 119.07 ppm; IR (KBr): $\tilde{\nu}$ = 2972, 2890, 2237, 2197, 2137, 1648, 1489, 1466, 1190, 1097, 1057, 992, 944, 842, 794, 755, 667, 524 cm^{-1}; HRMS (ESI): *m*/*z* calcd for cation $C_8H_{17}N_2^+$: 141.1386 $[M]^+$, found: 141.1374; *m*/*z* calcd for $C_2N_3^-$: 66.0098 $[M]^-$, found: 66.0098.

1-Butyl-4-aza-1-azonia-bicyclo[2.2.2]octane dicyanamide (12b). Yield, 91.2%; colorless liquid; ^{1}H NMR (600 MHz, [D_6]DMSO): δ = 0.94 (t, 2H; CH_2), 1.32 (m, 2H; CH_2), 1.64 (m, 2H; CH_2), 3.02 (t, 6H; CH_2), 3.17 (m, 2H; CH_2), 3.25 ppm (t, 6H; CH_2); ^{13}C NMR (600 MHz, [D_6]DMSO): δ = 13.42, 19.21, 22.93, 44.60, 51.47, 63.01, 119.01 ppm; IR (KBr): $\tilde{\nu}$ = 3485, 2962, 2890, 2226, 2189, 2129, 1463, 1378, 1306, 1096, 1057, 985, 903, 842, 793, 524 cm^{-1}; HRMS (ESI): *m*/*z* calcd for cation $C_{10}H_{21}N_2^+$: 169.1699 $[M]^+$, found: 169.1722; *m*/*z* calcd for $C_2N_3^-$: 66.0098 $[M]^-$, found: 66.0069.

1-Allyl-4-aza-1-azonia-bicyclo[2.2.2]octane dicyanamide (13b). Yield, 96.8%; colorless liquid; ^{1}H NMR (600 MHz, [D_6]DMSO): δ = 3.03 (t, 6H; CH_2), 3.26 (t, 6H; CH_2), 3.89 (d, 2H; CH_2), 5.62 (m, 2H; CH_2), 6.00 ppm (m, 1H; CH); ^{13}C NMR (600 MHz, [D_6] DMSO): δ = 44.63, 51.62, 65.25, 119.07, 125.35, 127.34 ppm; IR (KBr): $\tilde{\nu}$ = 2961, 2891, 2229, 2191, 2131, 1462, 1429, 1370, 1308, 1084, 1056, 992, 842, 639, 523 cm^{-1}; HRMS (ESI): *m*/*z* calcd for cation $C_9H_{17}N_2^+$: 153.1386 $[M]^+$, found: 153.1389; *m*/*z* calcd for $C_2N_3^-$: 66.0098 $[M]^-$, found: 66.0064.

1-(Prop-2-ynyl)-4-aza-1-azonia-bicyclo[2.2.2]octane dicyanamide (14b). Yield, 93.4%; white solid; ^{1}H NMR (600 MHz, [D_6] DMSO): δ = 3.07 (t, 6H; CH_2), 3.33 (m, 6H; CH_2), 4.13 (m, H; CH), 4.32 ppm (d, 2H; CH_2); ^{13}C NMR (151 MHz, [D_6]DMSO): δ = 44.59, 51.60, 52.68, 71.70, 84.21, 119.06 ppm; IR (KBr): $\tilde{\nu}$ = 3159, 3009, 2977, 2942, 2896, 2236, 2139, 2143, 1491, 1468, 1435, 1403, 1367, 1084, 1059, 989, 898, 799, 781, 753, 697, 661, 598, 513 cm^{-1}; HRMS (ESI): *m*/*z* calcd for cation $C_9H_{15}N_2^+$: 151.1230 $[M]^+$, found: 151.1245; *m*/*z* calcd for $C_2N_3^-$: 66.0098 $[M]^-$, found: 66.0066.

1-(Cyanomethyl)-4-aza-1-azonia-bicyclo[2.2.2]octane dicyanamide (15b). Yield, 89.1%; white solid; ^{1}H NMR (600 MHz, [D_6] DMSO): δ = 3.10 (t, 6H; CH_2), 3.41 (t, 6H; CH_2), 4.80 ppm (s, 2H; CH_2); ^{13}C NMR (151 MHz, [D_6]DMSO): δ = 44.47, 50.32, 52.69, 111.51, 119.06 ppm; IR (KBr): $\tilde{\nu}$ = 3319, 3021, 2961, 2892, 2239, 2198, 2136, 1463, 1376, 1318, 1103, 1056, 993, 944, 840, 795, 669, 523 cm^{-1}; HRMS (ESI): *m*/*z* calcd for cation $C_9H_{17}N_2^+$: 152.1183 $[M]^+$, found: 152.1182; *m*/*z* calcd for $C_2N_3^-$: 66.0098 $[M]^-$, found: 66.0067.

1-(2-Hydroxyethyl)-4-aza-1-azonia-bicyclo[2.2.2]octane dicyanamide (16b). Yield, 97.6%; white solid; ^{1}H NMR (600 MHz, [D_6] DMSO): δ = 3.03 (t, 6H; CH_2), 3.31 (m, 2H; CH_2), 3.37 (t, 6H; CH_2), 3.85 (t, 2H; CH_2), 5.28 ppm (t, 6H; CH_2); ^{13}C NMR (151 MHz, [D_6]DMSO): δ = 44.65, 52.41, 54.09, 65.30, 119.06 ppm; IR (KBr): $\tilde{\nu}$ = 3489, 3139, 3001, 2966, 2933, 2892, 2232, 2194, 2136, 1482, 1459, 1373, 1307, 1103, 1058, 991, 903, 886, 834, 793, 599, 521, 409 cm^{-1}; HRMS (ESI): *m*/*z* calcd for cation $C_8H_{17}N_2O^+$: 155.1543 $[M]^+$, found: 155.1540; *m*/*z* calcd for $C_2N_3^-$: 66.0098 $[M]^-$, found: 66.0065.

X-ray analysis

The single crystal X-ray diffraction data collections were carried out on a Rigaku AFC-10/Saturn 724+ CCD diffractometer with graphite-monochromated Mo Kα radiation (λ = 0.71073 Å) using the multi-scan technique. The structures were determined by direct methods using SHELXS-97 and refined by full-matrix least-squares procedures on F^2 with SHELXL-97.[25] All non-hydrogen atoms were obtained from the difference Fourier map and subjected to anisotropic refinement by full-matrix least squares on F^2.[26]

A colorless crystal of **15b** which suitable for single crystal X-ray diffraction was obtained by slow evaporation of its solutions with the mixture of CH_3OH and ethyl acetate. The structure is shown in the Fig. 1. According to the X-ray crystallographic analysis, **15b** crystallized in monoclinic space group $p2_{(1)}/n$ with a calculated density of 1.36 g cm^{-3} (−120.2 °C). The crystallographic data and refinement details are given in Table 1.

Calculation procedure

Calculations were performed with the Gaussian 09 suite of programs.[27] The geometric optimization of the structures was carried out by using the B3LYP functional with the 6-31++G** basis set,[28] and single energy points were calculated at the MP2/6-311++G** level. For the cations of ILs, their optimized structures were characterized to be true local-energy minima on the potential-energy surface without imaginary frequencies. The molecular volumes were calculated by keyword "volume". Electron density is 0.001 electrons per bohr^3, but the random points were increased to 2000. Heats of formation (HOF) of ILs are calculated based on the Born–Haber energy cycle.

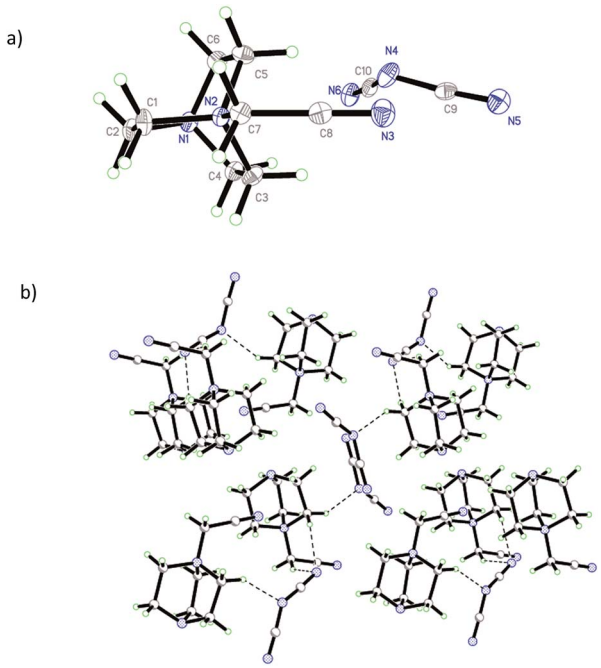

Fig. 1 (a) Thermal ellipsoid plot (30%) and labeling scheme for **15b**; (b) ball-and-stick packing diagram of **15b**.

Table 1 Crystallographic data and structure determination parameters for **15b**

	15b
Formula	$C_{10}H_{15}N_6$
CCDC number	1509452
Mr	219.28
Cristal size	0.25 × 0.21 × 0.20
Cristal system	Monoclinic
Space group	$P2_{(1)}/n$
T [K]	153(2)
a [Å]	7.008(14)
b [Å]	14.392(3)
c [Å]	10.586(2)
V [Å^3]	1071.4(4)
Z	4
ρ_{calcd} [g cm^{-3}]	1.360
μ [mm^{-1}]	0.090
F (000)	468
α [°]	90
β [°]	97.40(3)
γ [°]	90
θ [°]	2.40 to 27.48
Index range	$-8 \leq h \leq 9$
	$-18 \leq k \leq 18$
	$-13 \leq l \leq 12$
Reflections collected	7726
Independent reflections (R_{int})	2462(0.0378)
Data/restraints/parameters	2462/0/145
GOF on F^2	1.197
R_1 [$I > 2\sigma(I)$][a]	0.0643
wR_2 [$I > 2\sigma(I)$][b]	0.1476
R_1 [all data]	0.0716
wR_2 [all data]	0.1592
Largest diff. peak and hole [e Å^{-3}]	0.234 and −0.651

[a] $R_1 = \Sigma||F_o| - |F_c||/\Sigma|F_o|$. [b] $wR_2 = \{[\Sigma w(F_o^2 - F_c^2)^2]/\Sigma[w(F_o^2)^2]\}^{1/2}$.

HOF of the cations were obtained by using the method of isodesmic reactions. HOF of the anion ($N(CN)_2^-$) is literature values.[29] The enthalpy of reaction ΔH_r^o was obtained by combining the MP2/6-311++G** energy difference for the reaction, the scaled zero-point energies, and other thermal factors. Based on HOF and density values, the specific impulses of ILs were calculated using Explo 5 program.

Results and discussion

The ABCO and DABCO-based ILs were synthesized by a two-step method including quaternization and metathesis reactions (Scheme 1). The resulting ILs were characterized by ^{1}H and ^{13}C NMR, IR spectroscopies, and ESI-MS, which well support the structures of ILs. The properties of ILs (**9–16**) were measured or calculated (Table 2), including phase transition temperature (T_m or T_g), decomposition temperature (T_d), viscosity (η), density (ρ), ignition delay time (t_{id}), heat of formation (ΔH_f) and specific impulse (I_{sp}).

Thermal properties of ILs mainly include T_m (or T_g) and T_d, these were determined by differential scanning calorimetric (DSC) measurements with a heating rate of 10 °C min^{-1}. As shown in Table 2, the ABCO-based ILs of **10a**, **12a**, **13a** and **16a** melt below room temperature as 2.7, 22.7, 16.5 and 19.7 °C, respectively. For the DABCO-based ILs, **12b**, **13b** and **16b** is liquid at room temperature with T_m (or T_g) as 2.0, −80.8 and −71.8 °C. The T_d of ABCO-based ILs range from 230.7 (**15a**) to 322.0 °C (**10a**), and DABCO-based ILs from 207.5 (**15b**) to 281.3 °C (**9b**). Based on Fig. 2, it is clearly seen that ABCO-based ILs exhibit higher thermal stabilities than DABCO-based ILs. Moreover, the ILs with alkyl substituents (–CH_3, –C_2H_5, –C_3H_7 and –C_4H_9) are thermally stable up to 275.2 °C while the ILs with substituents (–CH_2CCH and –CH_2CN) become much less stable with T_d as 236.0 (**14a**), 208.2 (**14b**), 230.7 (**15a**) and 207.5 °C (**15b**), respectively.

Density is the key parameter of high-density-energy materials (HDEM) like propellant fuels, which affects I_{sp} values of propellants and fuel loading of rockets. For the resulting N-based ILs, densities are all bigger than 1.00 g cm^{-3} varying from 1.06 to 1.31 g cm^{-3} (Table 2), whereas the densities of BH-anion ILs are all less than 1.03 g cm^{-3} such as [Bmim]BH_4

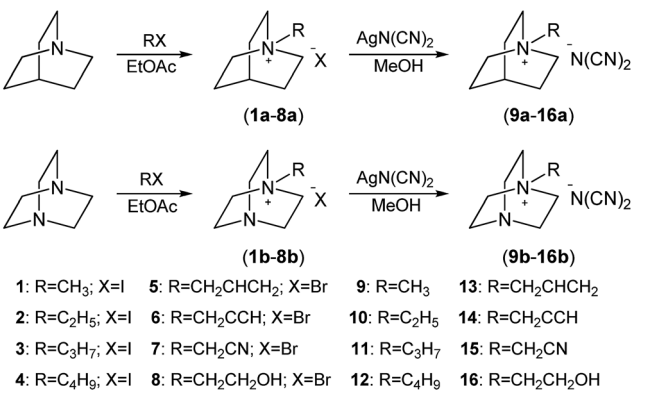

Scheme 1 Synthesis of ABCO and DABCO-based ILs.

Table 2 Physicochemical properties of the ILs

ILs	T_m[a] [°C]	T_d[b] [°C]	ρ[c] [g cm^{-3}]	μ[d] [mPa s]	ΔH_f[e] [kJ mol^{-1}]	IS[f] [J]	FS[g] [N]	I_{sp}[h] [s]	t_{id}[i] [ms]
9a	35.3	317.8	1.16	—	154.4	>60	>360	262.3	34
10a	2.7	322.0	1.09	50.1	136.9	>60	>360	262.0	63
11a	76.0	320.7	1.14	—	123.7	>60	>360	261.6	29
12a	22.7	318.0	1.06	74.4	116.9	>60	>360	261.3	100
13a	16.5	303.0	1.10	44.9	254.9	>60	>360	263.1	49
14a	64.8	236.0	1.19	—	431.1	>60	>360	265.2	14
15a	99.0	230.7	1.27	—	356.7	>60	>360	263.2	—
16a	19.7	275.5	1.16	192.0	7.8	>60	>360	262.0	186
9b	50.8	281.3	1.20	—	265.8	>60	>360	263.8	39
10b	37.0	280.8	1.17	—	240.6	>60	>360	264.1	82
11b	55.3	276.8	1.17	—	232.3	>60	>360	264.2	106
12b	2.0	275.2	1.10	195.5	223.2	>60	>360	264.0	120
13b	−80.8[j]	264.3	1.14	141.7	366.3	>60	>360	265.1	67
14b	105.8	208.2	1.25	—	537.5	>60	>360	266.2	20
15b	127.8	207.5	1.31	—	469.0	>60	>360	261.7	—
16b	−71.8[j]	260.2	1.22	594.3	113.9	>60	>360	260.5	1053

[a] Melting point (peak point). [b] Decomposition temperature (peak point). [c] Density (25 °C). [d] Viscosity (25 °C). [e] Heat of formation. [f] Impact sensitivity. [g] Friction sensitivity. [h] Specific impulse (Explo5 v6.02. IL/WFNA = 24/76, w/w; isobaric conditions, equilibrium expansion, 7.0 MPa chamber pressure). [i] Ignition delay time (WFNA). [j] Glass-transition temperature.

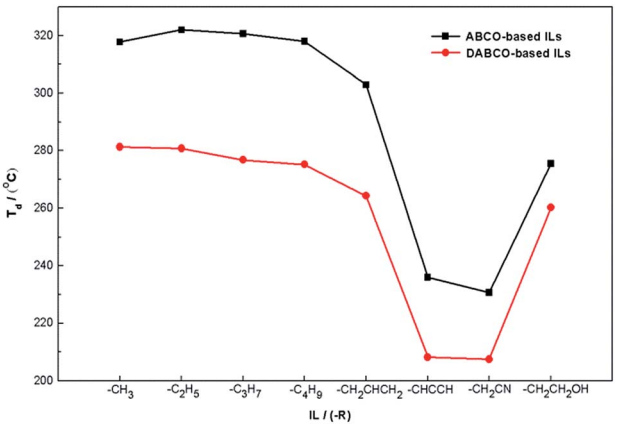

Fig. 2 Variation in decomposition temperatures of ILs with *R* substituents.

(0.91 g cm^{-3}),[10] [Bmim]BH_3CN (0.97 g cm^{-3}),[12] and [Bmim]$BH_2(CN)_2$ (0.96 g cm^{-3}),[14] respectively. As to cations, bicyclic ammonium cations were chosen rather than the common imdazolium-based cations. Based on Fig. 3, it show that DABCO-based ILs possess higher densities than the corresponding ABCO-based ILs. In other words, ILs become denser by substituting C with N atom in the cations. For the same series, the ILs with function groups (–CCH, –CN and –OH) exhibit the higher densities as 1.19 (**14a**), 1.27 (**15a**), 1.16 (**16a**), 1.25 (**14b**), 1.31 (**15b**) and 1.22 g cm^{-3} (**16b**), respectively.

Furthermore, **9a** and **14b** were targeted for the comparison with their corresponding isomers, shown in Fig. 4. With the same $N(CN)_2^-$ anion, the two pairs of isomers have the different structures of cations. The results show that **9a** (1.20 g cm^{-3}) and **14b** (1.19 g cm^{-3}) possess higher densities than the corresponding pyrrolidinium and imidazolium ILs (1.05 and 1.07 g cm^{-3}).[30,31] It indicates that bicyclic ABCO and DABCO cations contribute to the higher densities of ILs than monocyclic pyrrolidinium and imidazolium. Also, the molecular volumes of four cations were calculated (Fig. 4). The molecular volumes of ABCO (1766.554 bohr^3) and DABCO (1953.010 bohr^3) are smaller than the corresponding pyrrolidinium (1845.543 bohr^3) and imidazolium (2021.264 bohr^3) isomers, which are consistent with the experiments.

Heats of formation (HOF) of ILs were calculated based on a Born–Haber energy cycle (Scheme 2). The following equations were used for the HOF calculations.[32–34]

$$\Delta H_f^\circ \text{ (ionic salt, 298 K)} = \Delta H_f^\circ \text{ (cation, 289 K)} + \Delta H_f^\circ \text{ (anion, 289 K)} - \Delta H_L \quad (1)$$

$$\Delta H_L = U_{POT} + [p(n_M/2 - 2) + q(n_x/2 - 2)]RT \quad (2)$$

$$U_{POT} = \gamma(\rho_m/M_m)^{1/3} + \delta \quad (3)$$

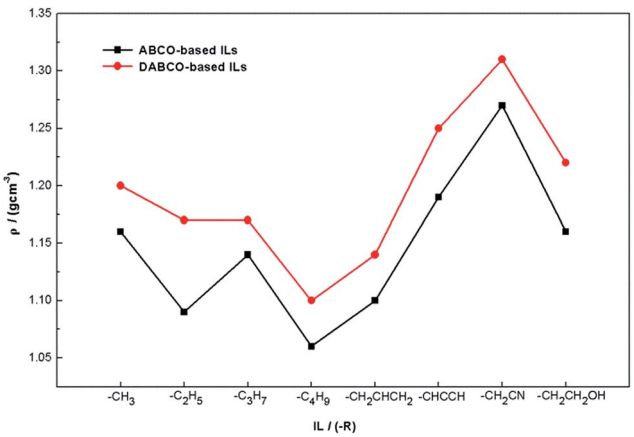

Fig. 3 Variation in densities of ILs with *R* substituents.

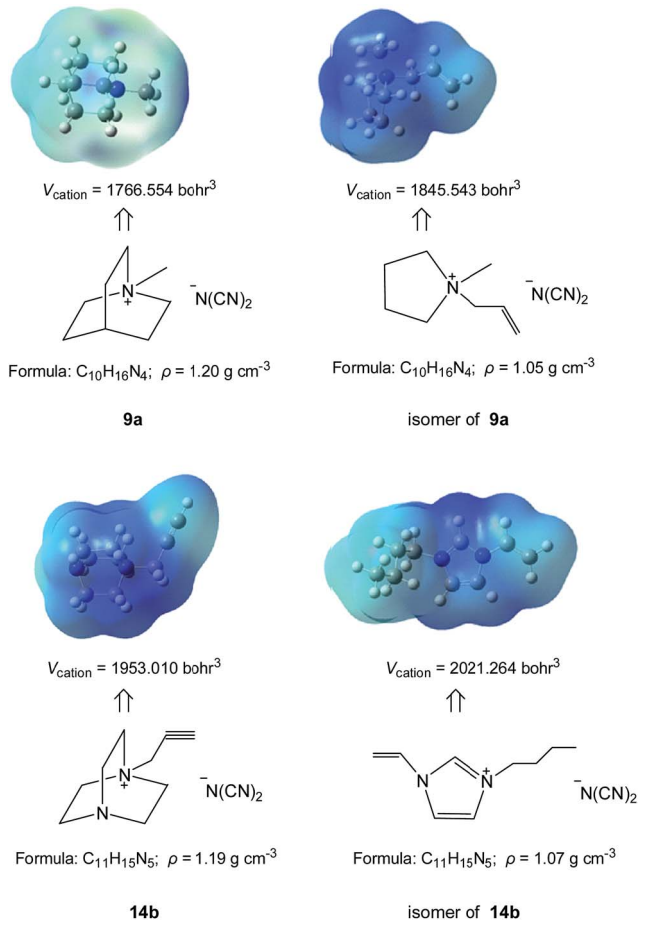

Fig. 4 Comparison of **9a** and **14b** with their corresponding isomers.

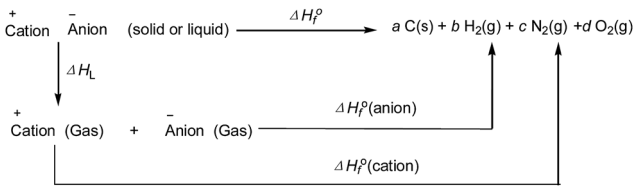

Scheme 2 Born–Haber cycle for the formation of ILs.

where ΔH_L is the lattice energy of ILs, kJ mol^{-1}; U_{POT} the lattice potential energy, kJ mol^{-1}; ρ_m the density, g cm^{-3}; M_m the formula mass of salts; the values for p, q, γ, and δ are taken from the literature.[32]

HOF of cations in the gas phase were calculated by using the Gaussian 09 suite of programs, HOF of $N(CN)_2^-$ was taken from the literature data,[29] and lattice energies were calculated with eqn (2). From Table 2, it shows that HOF of the ABCO-based and DABCO-based ILs vary from 7.8 to 431.1 and from 113.9 to 537.5 kJ mol^{-1}. Based on Fig. 5, it can be seen that HOF changes of the two series of ILs follow the same trend. ILs with $-CH_2CCH$ and $-CH_2CH_2OH$ substituents have the highest and the lowest HOF. With HOF and density values in hand, the specific impulses were calculated by using Explo 5 program. The specific impulses

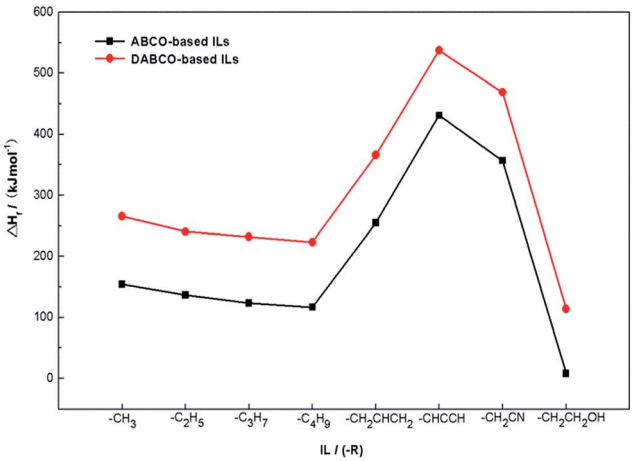

Fig. 5 Variation in HOF of ILs with *R* substituents.

of ILs range from 260.5 to 266.2 s, especially **14b** possessing the biggest value of 266.2 s.

Ignition delay time (t_{id}) is the critical parameter in determining whether fuels could be suitable for hypergolic bipropellants. Droplet tests with WFNA as the oxidizer were employed to measure the t_{id} of ILs. The typical test procedure is as follows: (1) a droplet of sample IL (about 50 μL) was dropped into a 10 mL glass breaker containing an excess amount of WFNA (1.5 mL); (2) a high-speed camera operating at 1000 frames per s was used to record the t_{id} which is measured as the time from initial contact between the sample and WFNA to appearance of a flame. A sequence of pictures of **10a** and **13a** into WFNA was depicted in Fig. 6, thereby demonstrating that the hypergolic ILs can undergo self-sustained combustion after ignition. The results exhibit that the ILs are hypergolic with WFNA except for **15a** and **15b** (Table 2). Among these ILs, **11a**, **14a** and **14b** are excellent hypergolic materials with t_{id} at 29, 14 and 20 ms, respectively. Compared with DABCO-based ILs, ABCO-based ILs exhibit a shorter t_{id}. However, in the same

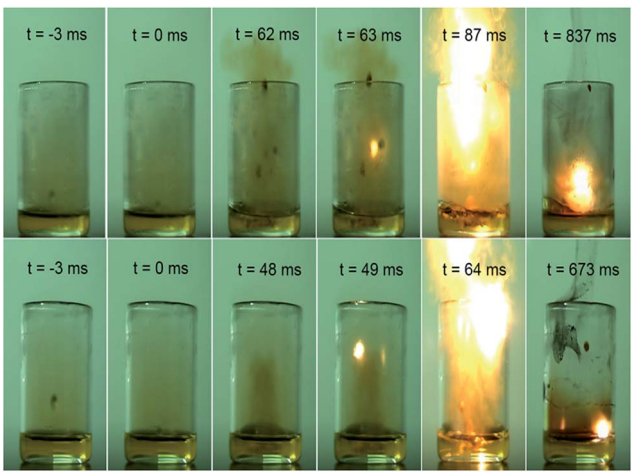

Fig. 6 Ignition delay times recorded by a high-speed camera (1000 frames per s) of **10a** (top) and **13a** (bottom).

series, the changes of IL's t_{id} do not follow a clear trend because of the interactive factors including thermal stability, viscosity, reactivity, and so on.

Conclusion

Two series of ABCO/DABCO-based ILs were synthesized in good yields through quaternization and metathesis reactions. The resulting bicyclic ammonium ILs were confirmed by ^{1}H and ^{13}C NMR, IR spectroscopies, and ESI-MS. Their key properties such as T_m (or T_g), T_d, ρ, η, ΔH_f, I_{sp} and t_{id} were measured or calculated. The results show that DABCO-based ILs possess lower decomposition temperature, higher density and bigger specific impulse than the corresponding ABCO-based ILs. Cations with substituents can tune properties of the resulting ILs as follows: (1) the ILs with alkyl substituents ($-CH_3$, $-C_2H_5$, $-C_3H_7$, $-C_4H_9$) are thermally stable up to 260 °C while the ILs with substituents ($-CH_2CCH$ and $-CH_2CN$) become much less stable with T_d as low as 208.2 and 207.5 °C; (2) ILs with dense function groups (–CCH, –CN, –OH) exhibit higher densities as 1.19 (**14a**), 1.27 (**15a**), 1.16 (**16a**), 1.25 (**14b**), 1.31 (**15b**), 1.22 g cm^{-3} (**16b**), respectively; (3) ILs with $-CH_2CCH$ and $-CH_2OH$ substituents have the highest and lowest HOF. Moreover, compared with the corresponding pyrrolidinium- and imidazolium-based isomers (1.05 and 1.07 g cm^{-3}), 1-methyl-1-azonia-bicyclo[2.2.2]octane and 1-(prop-2-ynyl)-4-aza-1-azonia-bicyclo[2.2.2]octane dicyanamide possess higher densities as 1.20 (**9a**) and 1.19 g cm^{-3} (**14b**), which are consistent with our expectation. With I_{sp} (260.5–266.2 s) and t_{id} (14–1053 ms), the ABCO/DABCO-based ILs have potential applications as the dense bipropellant fuels.

Acknowledgements

The authors gratefully acknowledge the support from National Natural Science Foundation of China (21376252, 21576270, 21676281); National Key Projects for Fundamental Research and Development of China (2016YFB0600903).

Notes and references

1 A. Osmont, L. Catoire, T. M. Klapötke, G. L. Vaghjiani and M. T. Swihart, *Propellants, Explos., Pyrotech.*, 2008, **33**, 209–212.
2 S. G. Kulkarni, V. S. Bagalkote, S. S. Patil, U. P. Kumar and V. A. Kumar, *Propellants, Explos., Pyrotech.*, 2009, **34**, 520–525.
3 C. B. Jones, R. Haiges, T. Schroer and K. O. Christe, *Angew. Chem., Int. Ed.*, 2006, **45**, 4981–4984.
4 P. D. McCrary, P. A. Beasley, O. A. Cojocaru, S. Schneider, T. W. Hawkins, J. P. L. Perez, B. W. McMahon, M. Pfeil, J. A. Boatz, S. L. Anderson, S. F. Son and R. D. Rogers, *Chem. Commun.*, 2012, **48**, 4311–4313.
5 P. D. McCrary, P. A. Beasley, S. A. Alaniz, C. S. Griggs, R. M. Frazier and R. D. Rogers, *Angew. Chem., Int. Ed.*, 2012, **51**, 9784–9787.
6 S. Schneider, T. Hawkins, M. Rosander, G. Vaghjiani, S. Chambreau and G. Drake, *Energy Fuels*, 2008, **22**, 2871–2872.
7 S. Schneider, T. Hawkins, M. Rosander, J. Mills, G. Vaghjiani and S. Chambreau, *Inorg. Chem.*, 2008, **47**, 6082–6089.
8 K. Wang, Y. Zhang, D. Chand, D. A. Parrish and J. M. Shreeve, *Chem.–Eur. J.*, 2012, **18**, 16931–16937.
9 Q. Zhang and J. M. Shreeve, *Chem.–Eur. J.*, 2013, **19**, 15446–15451.
10 S. Li, H. Gao and J. M. Shreeve, *Angew. Chem., Int. Ed.*, 2014, **53**, 2969–2972.
11 Q. Zhang, P. Yin, J. Zhang and J. M. Shreeve, *Chem.–Eur. J.*, 2014, **20**, 6909–6914.
12 Y. Zhang, H. Gao, Y.-H. Joo and J. M. Shreeve, *Angew. Chem., Int. Ed.*, 2011, **50**, 9554–9562.
13 Y. Zhang, Y. Huang, D. A. Parrish and J. M. Shreeve, *J. Mater. Chem. A*, 2011, **21**, 6891–6897.
14 Y. Zhang and J. M. Shreeve, *Angew. Chem., Int. Ed.*, 2011, **50**, 935–937.
15 D. Sengupta and G. L. Vaghjiani, *Propellants, Explos., Pyrotech.*, 2015, **40**, 625.
16 T. Liu, X. Qi, S. Huang, L. Jiang, J. Li, C. Tang and Q. Zhang, *Chem. Commun.*, 2015, **10**, 2031–2034.
17 S. Schneider, T. Hawkins, Y. Ahmed, M. Rosander, L. Hudgens and J. Mills, *Angew. Chem., Int. Ed.*, 2011, **50**, 5886–5888.
18 Q. Zhang and J. M. Shreeve, *Chem. Rev.*, 2014, **114**, 10527–10574.
19 Q. Zhang, Z. Li, J. Zhang, S. Zhang, L. Zhu, J. Yang, X. Zhang and Y. Deng, *J. Phys. Chem. B*, 2007, **111**, 2864–2872.
20 J. Y. Kazock, M. Taggougui, B. Carré, P. Willmann and D. Lemordant, *Synthesis*, 2007, **24**, 3776–3778.
21 Y. Cai, *Acta Crystallogr., Sect. C: Cryst. Struct. Commun.*, 2011, **67**, m13–m16.
22 I. W. Wyman and D. H. Macartney, *Org. Biomol. Chem.*, 2010, **8**, 253–260.
23 N. Maras, S. Polanc and M. Kocevar, *Org. Biomol. Chem.*, 2012, **10**, 1300–1310.
24 A. Khalafi-Nezhad and S. Mohammadi, *Synthesis*, 2012, **44**, 1725–1735.
25 G. M. Sheldrick, *SHELXTL V5.1 Software Reference Manual*, Bruker AXS Inc., Madison, Wisconsin, USA, 1997.
26 G. M. Sheldrick, *Program for Semiempirical Absorption Correction of Area Detector Data*, 1996.
27 M. J. Frisch, G. W. Trucks, H. B. Schlegel, G. E. Scuseria, M. A. Robb, J. R. Cheeseman, G. Scalmani, V. Barone, B. Mennucci, G. A. Petersson, H. Nakatsuji, M. Caricato, X. Li, H. P. Hratchian, A. F. Izmaylov, J. Bloino, G. Zheng, J. L. Sonnenberg, M. Hada, M. Ehara, K. Toyota, R. Fukuda, J. Hasegawa, M. Ishida, T. Nakajima, Y. Honda, O. Kitao, H. Nakai, T. Vreven, J. A. Montgomery Jr, J. E. Peralta, F. Ogliaro, M. Bearpark, J. J. Heyd, E. Brothers, K. N. Kudin, V. N. Staroverov, T. Keith, R. Kobayashi, J. Normand, K. Raghavachari, A. Rendell, J. C. Burant, S. S. Iyengar, J. Tomasi, M. Cossi, N. Rega, J. M. Millam, M. Klene, J. E. Knox, J. B. Cross, V. Bakken, C. Adamo, J. Jaramillo, R. Gomperts, R. E. Stratmann,

O. Yazyev, A. J. Austin, R. Cammi, C. Pomelli, J. W. Ochterski, R. L. Martin, K. Morokuma, V. G. Zakrzewski, G. A. Voth, P. Salvador, J. J. Dannenberg, S. Dapprich, A. D. Daniels, O. Farkas, J. B. Foresman, J. V. Ortiz, J. Cioslowski and D. J. Fox, Gaussian, Inc., Wallingford CT, 2013.

28 R. G. Parr and W. Yang, *Density Functional Theory of Atoms and Molecules*, Oxford University Press, New York, 1989.

29 H. Gao, Y. H. Joo, B. Twamley, Z. Zhou and J. M. Shreeve, *Angew. Chem., Int. Ed.*, 2009, **48**, 2792–2795.

30 P. Li, D. R. Paul and T. S. Chung, *Green Chem.*, 2012, **14**, 1052–1063.

31 N. Cai, J. Zhang, D. Zhou, Z. Yi, J. Guo and P. Wang, *J. Phys. Chem. C*, 2009, **113**, 4215–4221.

32 H. D. B. Jenkins, H. K. Roobottom, J. Passmore and L. Glasser, *Inorg. Chem.*, 1999, **38**, 3609–3620.

33 B. Rice, E. Byrd and W. Mattson, *High Energy Density Materials*, 2007, **125**, 153–194.

34 A. Schmidt, A. S. Lindner and F. J. Ramirez, *J. Mol. Struct.*, 2007, **834**, 311–317.